

Dynamics and morphology of polyolefinic elastomers by means of ^{13}C and ^1H solid-state n.m.r.

M. Geppi*, F. Ciardelli[†] and C. A. Veracini

Dipartimento di Chimica e Chimica Industriale, v. Risorgimento 35, 56126 Pisa, Italy

and C. Forte

Istituto di Chimica Quantistica ed Energetica Molecolare–CNR, v. Risorgimento 35, 56126 Pisa, Italy

and G. Cecchin and P. Ferrari

Centro Ricerche Montell 'G. Natta', P.le Privato G. Donegani 12, 44100 Ferrara, Italy

(Received 22 May 1996; revised 20 November 1996)

An extensive study of both ^1H and ^{13}C T_1 (spin-lattice) and $T_{1\rho}$ (spin-lattice in the rotating frame) relaxation times as well as T_{CH} (proton–carbon cross-polarisation times) was undertaken in order to investigate the morphology and dynamics of an ethylene/propylene/ethylidene–norbornene terpolymer and two ethylene/propylene random copolymers obtained using different catalytic systems. Several selective n.m.r. techniques were first used in order to obtain information on the structure and phase composition of the three copolymers. Two of the samples were found to consist of a single phase, whereas the copolymer obtained with a Ti-based catalyst clearly showed three phases: rubbery ethylene/propylene random copolymer, crystalline polyethylene, and isotactic crystalline polypropylene. Moreover, a fourth phase, made of 'rigid' amorphous polyethylene, bordering the crystalline polyethylenic regions, was singled out by means of ^1H T_1 , ^{13}C $T_{1\rho}$ and T_{CH} measurements. In the same sample the dimensions of the crystalline domains dispersed in the rubber matrix were roughly estimated on the basis of the proton relaxation times. Qualitative and semi-quantitative information on motions in the kHz and MHz ranges was derived from carbon relaxation times. © 1997 Elsevier Science Ltd.

(Keywords: n.m.r.; relaxation times; polyolefins)

INTRODUCTION

High resolution solid-state nuclear magnetic resonance (n.m.r) is a powerful tool for studying the structural and dynamical properties of polymers. The possibility of easily performing selective experiments renders this spectroscopy particularly useful for the analysis of the different phases in heterogeneous polymers. Moreover, the relaxation times of both ^1H and ^{13}C nuclei contain a large amount of information on the dynamics; it must be pointed out, however, that a detailed analysis of the motional behaviour of polymeric systems is often very difficult.

Solid state n.m.r. has been employed previously to study ethylene/ α -olefin copolymers^{1–4} and, in particular, ethylene/propylene copolymers^{5,6}: in these works measurements of relaxation times, especially of nuclei belonging to crystalline phases, and selective experiments, which isolate phases with different mobility, were performed. The role played by the spin diffusion process in similar materials has also been investigated: Colquhoun and Packer⁴ have studied some copolymers of ethylene with α -olefins, with particular attention to

the correlation between spin diffusion and spin-lattice laboratory-frame and rotating-frame relaxation times of the signal arising from the crystalline region. More recently, Clayden⁷ has investigated the spin diffusion process in ethylene–propylene copolymers showing crystallizable ethylene. An estimate of the lamellar thickness of the different domains was obtained from the ^1H $T_{1\rho}$ values.

In this paper we report a ^1H and ^{13}C n.m.r. investigation of an ethylene/propylene/ethylidene–norbornene terpolymer and two ethylene/propylene random copolymers, obtained with different catalytic systems. In particular, we performed several experiments capable of revealing the phases present in each sample as well as characterizing them from the structural and dynamic points of view. The ^1H and ^{13}C spin-lattice (T_1) and spin-lattice in the rotating frame ($T_{1\rho}$) relaxation times and the cross-polarization times (T_{CH}) of all n.m.r. signals arising from each phase were measured and discussed qualitatively or using semi-quantitative models, thus gaining insight into the dynamics in the kHz and MHz ranges. In the case of one sample, which was found to consist of crystalline domains dispersed in a rubbery matrix, the relaxation times allowed us also to obtain information on the domain dimensions.

* Also at: Scuola Normale Superiore, Piazza Cavalieri, 56127 Pisa, Italy

[†] To whom correspondence should be addressed

EXPERIMENTAL

Samples

Three samples have been analysed: (I) an ethylene/propylene random copolymer obtained with a conventional vanadium-based catalyst (EPR-V); (II) an ethylene/propylene/ethylidene-norbornene random terpolymer obtained with a conventional vanadium-based catalyst (EPDM); and (III) an ethylene/propylene random copolymer obtained with a heterogeneous catalyst system based on MgCl₂-supported TiCl₄ and electron donors (EPR-Ti). Both EPR-V and EPDM samples are commercial products from Enichem Elastomeri (Italy), prepared by the slurry process, whereas EPR-Ti is an experimental product prepared by the gas phase process in the Montell Italia laboratories.

The main chemical-physical properties of the three copolymers are reported in Table 1. EPR-Ti exhibits both compositional heterogeneity and crystallinity, the latter confirmed by the presence in the d.s.c. thermogram of a melting peak at 123°C. In particular, its xylene-insoluble fraction consists of modified polyethylene plus about 3 wt% isotactic polypropylene (FT i.r.).

EPR-V and EPR-Ti have also been analysed by solution ¹³C n.m.r. and then submitted to fractionation by the solvent-gradient precipitation technique (heptane/methylethylketone mixtures). ¹³C n.m.r. analysis of the crude products showed, as expected, the presence of both regio (15%) and stereo irregularities (substantially atactic polypropylene runs) in the polypropylene sequences of EPR-V, whereas such irregularities were not detected in EPR-Ti. The apparent reactivity ratio products⁸ calculated for EPR-V and EPR-Ti are 0.6 and 2.0 respectively.

Fractionation data show a relatively broad chemical composition distribution for both materials, the composition of the analysed fractions ranging from 40 to 66 wt% ethylene for EPR-V and from 30 to about 90 wt% ethylene for EPR-Ti.

N.m.r. measurements

The n.m.r. experiments were carried out on a Bruker AMX-300 WB spectrometer, working at 75.47 MHz for ¹³C, equipped with a 4 mm CP-MAS probe. The 90° proton pulse was 3.1 μs. The spin-lock field was 80 kHz. In the single pulse excitation (SPE) experiments we used a relaxation delay of 1 s. In the cross-polarization (CP) experiments we used a contact time of 2 ms for EPR-Ti and 3 ms for EPR-V and EPDM, and a relaxation delay

of 4 s for EPR-Ti and 2 s for EPR-V and EPDM. These parameters were chosen after suitable calibration experiments. ¹³C spin-lattice relaxation times were determined by means of Torchia's⁹ and inversion-recovery¹⁰ experiments. ¹³C spin-lattice relaxation times in the rotating frame were determined by means of a cross-polarization sequence followed by a variable carbon spin-lock time¹¹. ¹H spin-lattice relaxation times were determined through ¹³C observation by means of a ¹H inversion-recovery experiment followed by cross-polarization¹². ¹H spin-lattice relaxation times in the rotating frame were determined through ¹³C observation by means of a variable contact pulse experiment¹³. ¹H spin-spin relaxation times were determined through ¹³C observation by means of a modified cross-polarization sequence with a variable delay after the 90° pulse¹⁴. Proton-carbon cross-polarization times were determined using the 'inversion-recovery cross-polarization' (IRCP) sequence¹⁵, with a first cross-polarization time of 2 ms.

In the MAS experiments the spinning rate was always 3 kHz. All the experiments were performed at room temperature.

Because of the presence of numerous overlapping peaks in the spectra, all relaxation times were determined using the software 'SPORT-NMR'¹⁶, recently developed by some of us, in order to minimize errors arising from the superposition of peaks with different decay rates, thus obtaining distinct and accurate relaxation times for each individual signal.

RESULT AND DISCUSSION

Selective experiments

The ¹³C SPE-MAS and CP-MAS n.m.r. spectra of the three samples are shown in Figure 1. They have been interpreted on the basis of assignments in the literature^{8,17}. A complete interpretation of the ¹³C spectra is reported in Table 2.

The SPE-MAS spectra were recorded using a short relaxation delay in order to reveal contributions from mobile phases; the spectra of EPR-V and EPDM are very similar, whereas that of EPR-Ti shows relevant differences. Firstly, the latter spectrum does not show the peak at 35.2 ppm (peak *c*), corresponding to an S_{αβ} carbon arising from two adjacent propylene monomers with tail-to-tail insertion or from a propylene-ethylene-propylene monomer sequence with insertion head-to-head of the two propylene monomers; this indicates that, in contrast to EPR-V and EPDM, and in agreement with

Table 1 Composition and some chemical-physical properties of the three copolymers

Sample	Ethylene ^a (weight %)	\overline{M}_w^c	$\overline{M}_w/\overline{M}_n^c$	T_g^d (°C)	Crystallinity ^e (%)	Solubility in xylene ^g (weight %)	Ethylene content ^h (weight %)
EPR-V	56.5	199 000	6.5	-43	none	100	56.5
EPDM	46.6 ^b	195 000	4.1	-43	none	100	46.6
EPR-Ti	61.5	213 000	6.1	-41	12 ^f	76	50.0

^a FT i.r.

^b Ethylidene-norbornene content = 3.6 wt%

^c Gel permeation chromatography

^d DMTA

^e WAXS

^f From polyethylene runs

^g At room temperature

^h In the xylene soluble fraction

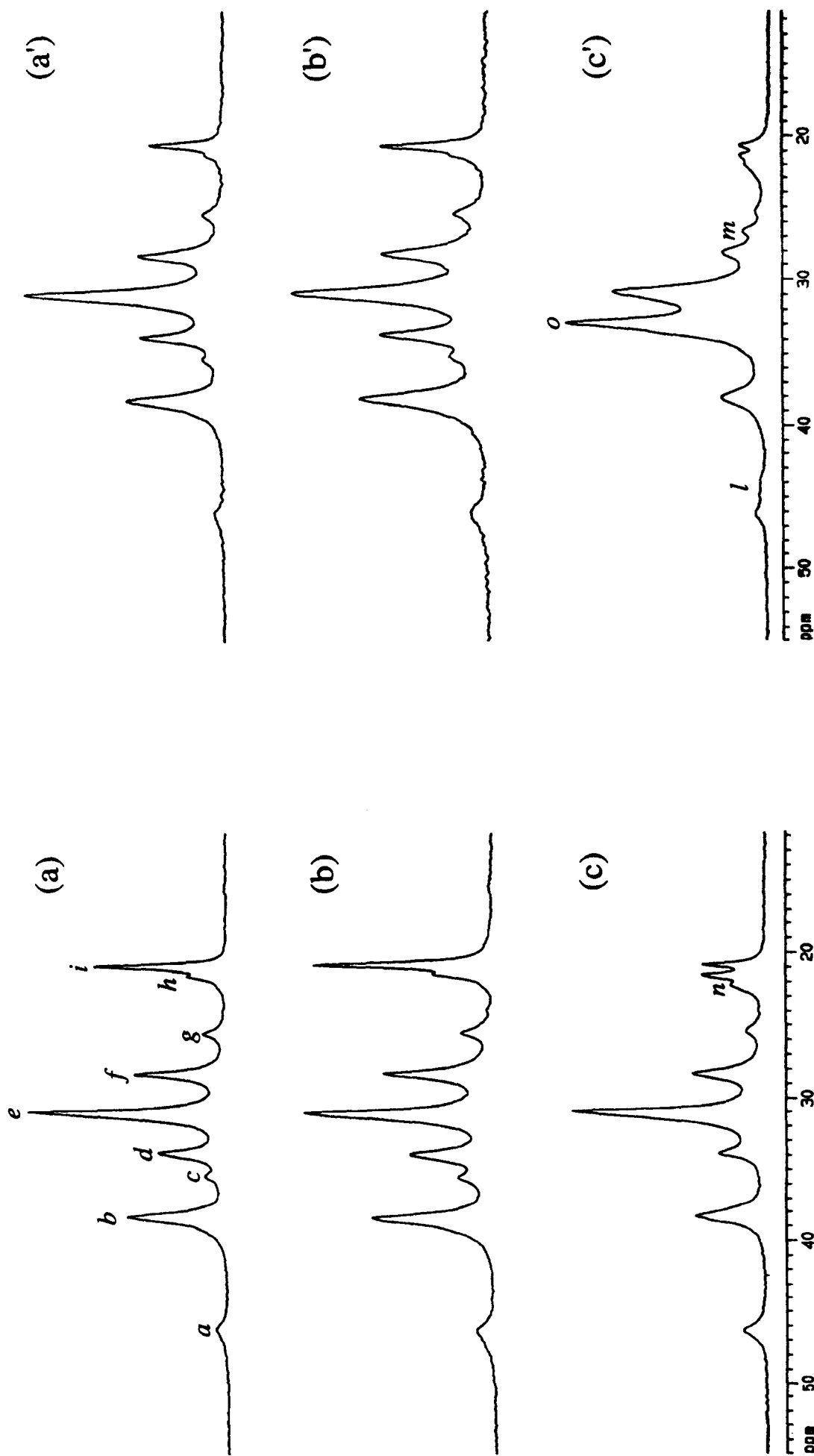


Figure 1 ^{13}C SPE-MAS (unprimed) and CP-MAS (primed) spectra of the three samples: (a) EPR-V, (b) EPDM and (c) EPR-Ti

Table 2 Assignment of the resonances in ^{13}C spectra of the three samples. The chemical shifts indicated are relative to tetramethylsilane (TMS). In the columns 'Carbon type' the capital letter refers to primary (P), secondary (S) or tertiary (T) carbons, whereas the Greek symbols denote the location of the nearest branch carbons and the superscript '+' a branch carbon equally or more distant than that indicated. In the column 'Monomer sequence' 'P' stands for the propylene monomer and 'E' for the ethylene monomer, and the asterisk indicates a tail-to-tail or head-to-head insertion of propylene monomers in the polymeric chain. In the column 'Phase' 'a' denotes amorphous and 'c' crystalline

Peak	Chemical shift	Carbon type	Monomer sequence	Phase
a	46.1	$\text{S}_{\alpha\alpha}$	PP	a
b	38.1	$\text{S}_{\alpha\gamma^+}$	PEP and PEE	a
c	35.2	$\text{S}_{\alpha\beta}$	PP* and PEP*	a
d	33.7	$\text{T}_{\gamma^+\gamma^+}$	EPE	a
e	30.9	$\text{T}_{\beta\gamma^+}$	PPE	a
		$\text{S}_{\gamma^+\gamma^+}$	EEE	a
f	28.2	$\text{S}_{\beta\gamma^+}$	EEP	a
		$\text{T}_{\beta\beta}$	PPP	a
g	25.3	$\text{S}_{\beta\beta}$	PEP	a
h	21.4	$\text{P}_{\beta\beta}$	PPP	a
i	20.7	$\text{P}_{\beta^+\gamma^+}$	EPE and PPE	a
l	44.6	$-\text{CH}_2-$	PPP	c
m	26.5	$>\text{CH}-$	PPP	c
n	22.1	$-\text{CH}_3$	PPP	c
o	33.0	$-\text{CH}_2-$	EEE	c

the solution ^{13}C n.m.r. results, EPR-Ti is very regio-regular.

The SPE-MAS and CP-MAS spectra for EPR-V and EPDM suggest that in these systems only one phase is present, consisting of rubbery ethylene-propylene random copolymer. Indeed, the two kinds of spectra have identical shape and the CP technique in both phases is not very efficient, the signal-to-noise ratio being smaller than in the SPE-MAS spectra. In contrast, the CP-MAS spectrum of EPR-Ti is markedly different from the corresponding SPE-MAS spectrum: the former shows peaks which are not present in the latter, namely those at 26.5, 33 and 44.6 ppm (peaks *m*, *o* and *l*, respectively), and a different shape of the methyl signals in the range 19.5–23.5 ppm. The intense peak at 33 ppm can be attributed to crystalline polyethylene, which shows the well-known low-field shift of about 2 ppm with respect to the non-crystalline polyethylene resonance, owing to the all-*trans* conformation¹⁸. The peaks at 26.5 and 44.6 ppm and the lowest field peak among the signals in the range 19.5–23.5 ppm have been attributed to methylene, methine and methyl carbons of crystalline polypropylene, respectively, as observed in isotactic polypropylene¹⁹. This is in agreement with the fact that these peaks are observed only in CP-MAS spectra. Thus, on the basis of what is observed in the SPE-MAS and CP-MAS spectra of EPR-Ti, we can suppose the presence in this system of three different phases: rubbery ethylene-propylene random copolymer, crystalline polyethylene, and crystalline isotactic polypropylene.

These experiments could not, however, exclude the presence of a rigid copolymeric phase in all the samples, as the signals observed in the ^{13}C SPE-MAS and CP-MAS spectra could arise, respectively, from a large quantity of mobile and a small quantity of rigid copolymer. Even static CP and SPE spectra, shown in Figure 2, cannot completely exclude the presence of a small quantity of a rigid copolymer phase. With the exception of the crystalline resonances in EPR-Ti (dotted peaks in the figure), which contribute to a very broad

peak in the static spectra, comparison of the ^{13}C SPE-MAS and CP-MAS spectra with the corresponding static spectra reveals that they are quite similar. Indeed, the static spectra show only a small broadening of the peaks, indicating a very high mobility of the phase, which can motionally average the chemical shift anisotropy even without magic angle spinning. This broadening, even if small, is sufficient to prevent a quantitative comparison between magic angle spinning and static spectra. Therefore we had to resort to other selective experiments. Several n.m.r. parameters could be used to distinguish between crystalline and amorphous polymeric phases, as the latter usually show shorter ^{13}C T_1 , ^1H $T_{1\rho}$ and longer cross-polarization time, T_{CH} , and ^1H T_2 . These parameters, however, do not depend on phase structure only; other factors, such as the type of carbon nucleus, local dynamics and proton spin diffusion, may not only be present but may also be preponderant. Carbon spin-lattice relaxation times can be influenced by particular local motions, whereas proton spin-lattice relaxation times T_1 and $T_{1\rho}$ are strongly affected by the spin diffusion process. T_{CH} and ^1H T_2 seemed more suitable for our aim since they are mainly dependent on proton-carbon dipolar interactions, much stronger in rigid than in mobile phases, and practically insensitive to the other effects.

The differences in ^1H T_2 were monitored by using a modified cross-polarization sequence in which a delay after the 90° pulse has been introduced⁵. In Figure 3 a series of spectra of EPR-Ti, obtained by varying the delay, is reported: the peaks at 26.5, 33 and 44.6 ppm (dotted in the figure) decay very rapidly and hence have a very short proton spin-spin relaxation time; this confirms that they arise from rigid phases. The other peaks show a noticeably slower decay; they must therefore be attributed to a mobile phase, with no evidence of the presence of a rigid copolymeric phase. The same experiment performed on EPR-V and EPDM showed a decay rate very similar to that of the mobile phase in EPR-Ti.

Unambiguous evidence of the absence of a rigid copolymer phase came from the variable contact pulse cross-polarization experiment, where the different build-up rate of magnetization at short contact pulses indicate different T_{CH} values. In Figure 4 a series of spectra for EPR-Ti, obtained at different contact times, is shown. As expected, at short contact pulses the peaks attributed to rigid phases, dotted in the figure, grow much faster than the others because of their more efficient carbon-proton dipolar interaction, whereas the build-up of magnetization for carbon nuclei belonging to the random copolymer was noticeably slower and similar to that observed in EPR-V and EPDM.

The phases identified by solid-state n.m.r. for the three samples are in agreement with the data for solubility in xylene and the percentage of crystallinity determined by WAXS, reported in Table 1.

Measurement of relaxation and cross-polarization times

As already mentioned in the previous section, relaxation times yield information on the dynamics, but also permit better characterization of the morphology in multiphase systems. To this end, several relaxation times were measured in the systems under investigation, i.e. spin-lattice (T_1) and spin-lattice in the rotating frame ($T_{1\rho}$) relaxation times for both carbon and proton nuclei, as well as proton-carbon cross-polarization times (T_{CH}).

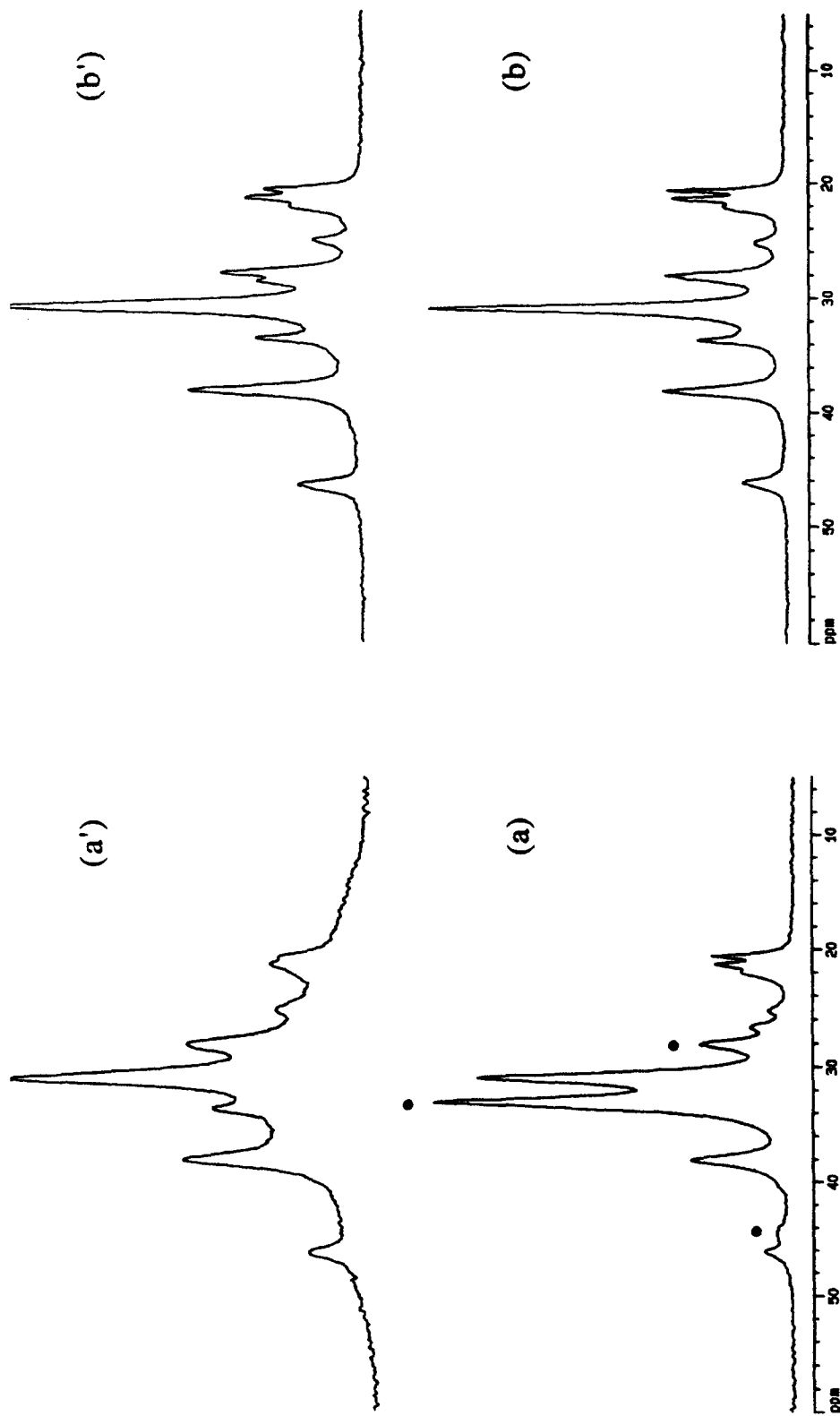


Figure 2 Comparison between MAS (unprimed) and static (primed) spectra of EPR-Ti: (a) ¹³C CP, (b) ¹³C SPE. Dots indicate peaks of particular interest discussed in the text

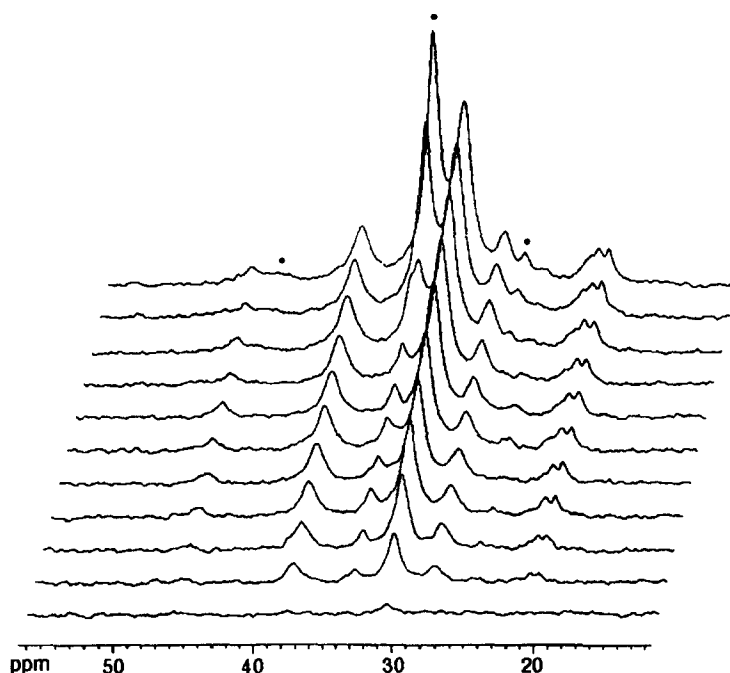


Figure 3 Series of proton T_2 selective spectra of EPR-Ti, obtained with the modified cross-polarization pulse sequence described in the text by varying the delay between $2\ \mu\text{s}$ (top spectrum) and $150\ \mu\text{s}$ (bottom spectrum). Dots indicate peaks of particular interest discussed in the text

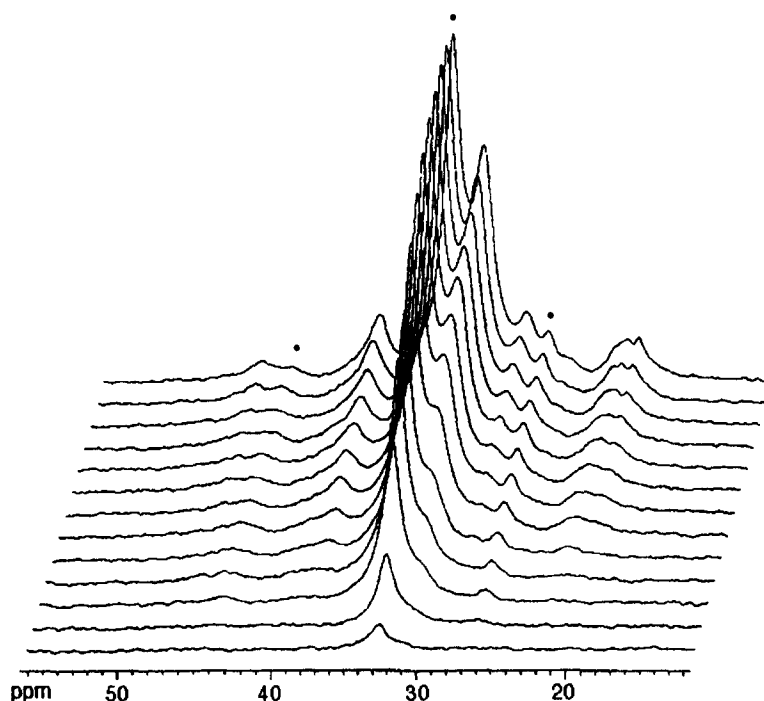


Figure 4 Series of spectra of EPR-Ti, obtained with the variable contact pulse cross-polarization sequence by varying the contact pulse time between $5\ \mu\text{s}$ (bottom spectrum) and $1\ \text{ms}$ (top spectrum). Dots indicate peaks of particular interest discussed in the text

Because of the high proton density usually present in organic polymers, proton spin-lattice relaxation times are generally strongly influenced by the spin diffusion process. However, even if these relaxation times do not give quantitative information on the dynamics, comparison of the values determined for the various phases of a heterophasic system gives an indication of the morphology. For carbon nuclei no significant spin diffusion takes place because of the high degree of isotopic dilution, except when the rigidity of the system allows relevant dipolar interactions even for diluted spins; therefore, in

non-rigid phases, carbon spin-lattice relaxation times depend exclusively on dynamic process in the MHz range, whereas spin-lattice relaxation in the rotating frame depends on motions in the mid-kHz range.

The strong overlap of peaks in the ^{13}C n.m.r. spectra, however, did not permit the measurement of relaxation times with the desired accuracy; this was particularly critical in the heterophasic sample, where peaks with very different relaxation times were often severely superimposed. With this aim we analysed our data using a new software, 'SPORT-NMR'¹⁶, which analytically

reproduces each spectrum of a series arising from a relaxation experiment as a sum of lorentzian and/or gaussian functions by means of a least-squares fitting procedure. Each peak in the completely relaxed spectrum was fitted using four parameters, i.e. the chemical shift, linewidth, gaussian percentage and intensity; in the remaining spectra of the series only the intensity of the peaks was varied in the fitting procedure. Relaxation times were determined by fitting the areas of the various peaks in the series, obtained from integration procedures, reported against the experimental variable delay employed in the pulse sequence, with suitable exponential functions. In this way we could obtain relaxation times for the individual peaks, thus being able to distinguish multi-exponential decays due to the overlap of peaks having different relaxation times from those peculiar to a single peak.

Proton spin-lattice relaxation times. The values of the proton spin-lattice relaxation times measured are reported in Table 3. As expected for single-phase systems, in which the proton spin diffusion process averages all ^1H spin-lattice relaxation times, in EPR-V and EPDM we obtained similar values for all the protons. It must be pointed out that the data which differ most are relative to the smallest peaks and therefore are affected by a larger error.

In EPR-Ti, protons belonging to the crystalline phases show higher values than protons of the mobile copolymeric phase. The values of the methyl protons do not align within experimental error to the values of the other protons: in the amorphous phase the methyl protons (peaks *h-i*) have slightly higher values when compared with the other protons of the same phase; in the crystalline phase (peak *n*) they have a noticeably shorter value with respect to non-methyl protons of the same phase, indicating a relevant contribution to proton relaxation from the internal rotation of the methyl group. Apart from these, the proton spin-lattice relaxation times within each phase have approximately the same values. Differently from EPR-V and EPDM, the value relative to peak *e*, which is well determined, is slightly but unequivocally higher than the values obtained for the other peaks of the rubbery phase; this can be explained only by assuming a contribution of a non-rubbery component.

Table 3 Proton spin-lattice relaxation times of the three samples. Values within parentheses indicate the experimental error relative to the last digit

Peak	Sample		
	EPR-V T_1 (ms)	EPDM T_1 (ms)	EPR-Ti T_1 (ms)
a	307 (20)	312 (40)	321 (20)
b	294 (3)	300 (5)	370 (15)
c	307 (20)	321 (40)	—
d	326 (6)	311 (6)	—
e	283 (3)	310 (4)	431 (7)
f	280 (7)	294 (6)	350 (10)
g	269 (10)	279 (20)	353 (20)
h-i	355 (10)	320 (5)	404 (35)
l	—	—	557 (40)
m	—	—	618 (40)
n	—	—	471 (10)
o	—	—	692 (15)

The theory of spin diffusion provides that in a time τ the mean square diffusive path length is

$$\langle x^2 \rangle = f D_S \tau \quad (1)$$

where the factor f is 4/3 for mono-dimensional spin diffusion (lamellar model)²⁰ and 6 for three-dimensional spin diffusion (spherical model)²¹. D_S is the diffusion coefficient, which can be roughly estimated from the ^1H spin-spin relaxation time T_2 , being²²:

$$D_S = \frac{0.13a^2}{T_2} \quad (2)$$

where a is the lattice constant. Since the parameter a is an ill-defined quantity in the case of polymeric systems, a modified expression, where a^2 is replaced with an average value of the square of distances between adjacent protons (\bar{a}^2), was derived²³. The value of \bar{a}^2 , calculated for polyethylene, is 4.66 \AA^2 ²³.

A measurement of the spin-spin relaxation times in the crystalline phases of EPR-Ti was obtained by using the pulse sequence described in the Experimental section¹⁴; a fit of the areas of the peaks arising from the crystalline phases with a gaussian function yielded a ^1H T_2 of $10.0 \pm 0.5 \mu\text{s}$. Therefore the diffusion coefficient D_S for the crystalline polyethylenic phase, obtained applying equation (2), comes to $6 \times 10^{-12} \text{ cm}^2 \text{ s}^{-1}$ and a value of the same order of magnitude is expected to be found for crystalline polypropylene.

A TEM analysis on EPR-Ti excluded the spherical model and has shown the presence of lamellar aggregates with average dimensions of the order of 1000 Å. The proton relaxation data, analysed on the basis of equation (1) within the lamellar model, indicate that the average linear dimension of the polyethylenic and polypropylenic domains in EPR-Ti are larger than 200–250 Å, in agreement with what is observed from the TEM analysis.

Proton spin-lattice relaxation times in the rotating frame. The values of proton spin-lattice relaxation times in the rotating frame are reported in Table 4.

The different values of proton $T_{1\rho}$ relative to different types of protons, found in both EPR-V and EPDM, were, in principle, not expected on the basis of their phase homogeneity. However, the great molecular mobility normally present in elastomeric systems at temperatures much higher than their glass transition temperature may render the proton spin diffusion process less efficient. This behaviour was previously observed, at room temperature, for other elastomers such as polybutyl acrylate²⁴, which has a glass transition temperature ($T_g = -46^\circ\text{C}$) similar to that of the ethylene/propylene random copolymers under investigation.

As is usually found, the protons having noticeably different values for ^1H $T_{1\rho}$ are those of methyl groups, which should be the most mobile groups because of their fast rotation around the ternary symmetry axis. For all types of protons it is true that

$$T_{1\rho}(\text{EPR-V}) > T_{1\rho}(\text{EPDM})$$

indicating different dynamic behaviour in the mid-kHz range for the two elastomers.

Since spin diffusion is usually efficient in crystalline phases, the $T_{1\rho}$ s of protons arising from the polypropylenic phase in EPR-Ti are very similar to each other;

Table 4 Proton spin-lattice relaxation times in the rotating frame of the three samples. Values within parentheses indicate the experimental error relative to the last digit. In the case of multiexponential behaviour the relative weights of the different exponentials are indicated

Peak	Sample			
	EPR-V	EPDM	EPR-Ti	
	$T_{1\rho}$ (ms)	$T_{1\rho}$ (ms)	$T_{1\rho}$ (ms)	weight %
a	5.4 (6)	4.5 (7)	5 (1)	
b	7.6 (1)	4.8 (1)	7.5 (2)	
c	10.3 (8)	4.5 (4)	—	
d	11.6 (2)	8.6 (3)	5.9 (5)	
e	7.8 (1)	5.2 (1)	7.5 (1)	
f	7.7 (2)	5.1 (1)	8.3 (3)	
g	7.3 (4)	5.3 (4)	9.5 (7)	
h	19 (2)	10 (2)	23 (2)	
i	24.6 (6)	23.7 (7)	25 (1)	
l	—	—	15 (3)	
m	—	—	15 (1)	
n	—	—	14 (1)	
o	—	—	4.8 (3)	45
	—	—	32 (1)	55

moreover, as expected on the basis of the large dimensions of the domains, the values obtained for the crystalline phases are different from those of protons belonging to the amorphous phase.

Carbon spin-lattice relaxation times. The ^{13}C spin-lattice relaxation times measured are reported in Table 5. In the case of EPR-Ti, both inversion-recovery and Torchia's pulse sequence were used to measure relaxation times arising from mobile and rigid phases, respectively.

Carbon spin-lattice relaxation times of amorphous phases are not strongly affected by spin diffusion²⁴; thus they can contain useful information on the molecular dynamics in the MHz region. In particular, for carbon nuclei belonging to very mobile phases, such as the elastomeric one, it is possible to explain relaxation data

Table 5 Carbon spin-lattice relaxation times of the three samples determined by means of inversion-recovery (Inv-Rec) pulse sequences. In the case of EPR-Ti the values obtained with Torchia's experiment are also reported. Values within parentheses indicate the experimental error relative to the last digit. In the case of multiexponential behaviour the relative weights of the different exponentials are indicated

Peak	Sample				
	EPR-V	EPDM	EPR-Ti		
	Inv-Rec	Inv-Rec	Inv-Rec	Torchia	weight %
T_1 (ms)	T_1 (ms)	T_1 (ms)	T_1 (s)		
a	193 (10)	189 (15)	182 (8)	—	
b	172 (1)	171 (1)	170 (2)	—	
c	159 (4)	157 (4)	—	—	
d	298 (3)	292 (3)	256 (7)	—	
e	244 (1)	241 (2)	254 (2)	—	
f	198 (2)	205 (2)	216 (2)	—	
g	167 (5)	166 (3)	171 (7)	—	
h	540 (20)	485 (30)	452 (15)	—	
i	458 (6)	470 (6)	467 (7)	—	
m	—	—	—	0.22 (4)	39
				15 (1)	61
n	—	—	409 (15)	—	
o	—	—	640 (40)	0.58 (8)	38
				25 (7)	23
				384 (40)	39

using simplified theoretical models, thus obtaining quantitative estimates of correlation times. In fact, for a carbon-13 nucleus relaxed by N directly bonded protons by means of a purely dipolar relaxation mechanism, assuming a monoexponential autocorrelation function and in the motional narrowing regime, the following relationship holds²⁵:

$$\tau_c = \frac{4.9 \times 10^{-11}}{NT_1} \quad (3)$$

where τ_c is the correlation time of the motion and an internuclear C-H distance of 1.09 Å has been assumed. Even though this model is highly simplified, it is often used for interpreting the experimental relaxation times of mobile phases in terms of dynamic effects.

The relaxation times measured for the methyl carbons are practically the same in the rubbery phases of the three samples, and are also similar to those of other ethylene-propylene random copolymers reported in the literature³; even though the backbone motions could in part affect relaxation²⁶, it is reasonable to consider that the main contribution arises from the rotation of the methyl group around the C_3 symmetry axis: the correlation time obtained for this motion, applying equation (3), is approximately 3.3×10^{-11} s for all the samples.

The same equation may be applied to the backbone carbons; in this case, if the segmental motions can be described by a single correlation time for the whole main chain and if this can be considered the main contribution to relaxation, following equation (3), all secondary carbons should have the same relaxation time and this should be half the relaxation time of tertiary carbons. If the values obtained for peaks *b* and *g* (see Table 5), which arise only from secondary carbons and, being quite intense, yield well determined relaxation times, are compared to the values obtained for peak *d*, relative to tertiary carbons, we find that the simple relation predicted by this model holds sufficiently well, considering possible motional heterogeneities; thus a correlation time for the segmental motions of about 1.6×10^{-10} s is determined. Correlation times of this order of magnitude were previously found for backbone motions of copolymers²⁵. In the case of EPR-Ti the agreement is less satisfactory, indicating a higher degree of motional heterogeneity in this sample.

The three-exponential decay of the signal belonging to crystalline polyethylene has been observed previously^{12,27} and the values that we have measured are within the ranges given by Kitamaru *et al.*¹² for the three different T_1 s. The relaxation behaviour of the crystalline phase can be explained by ^{13}C spin diffusional coupling of regions with very different intrinsic relaxation times, as discussed by Colquhoun and Packer⁴, even if the presence of motions like the 180°C rotation around the chain axis, supposed by Schröter and Posern to be responsible for the intermediate component²⁷, cannot be excluded.

Carbon spin-lattice relaxation times in the rotating frame. The measured carbon spin-lattice relaxation times in the rotating frame are reported in Table 6. In general, there are two contributions to this type of relaxation, one arising from spin-lattice processes and the other from spin-spin ones¹¹. When the spin-spin relaxation pathway plays an important role, the ^{13}C

Table 6 Carbon spin-lattice relaxation times in the rotating frame of the three samples. Values within parentheses indicate the experimental error relative to the last digit. In the case of multiexponential behaviour the relative weights of the different exponentials are indicated

Peak	Sample					
	EPR-V		EPDM		EPR-Ti	
	$T_{1\rho}$ (ms)	weight %	$T_{1\rho}$ (ms)	weight %	$T_{1\rho}$ (ms)	weight %
a	5.3 (3)		4.8 (4)		—	
b	3.2 (1)	52	2.3 (2)	53	2.3 (2)	42
	16.4 (8)	48	13 (1)	47	11.1 (7)	58
c	9.9 (6)		3.1 (6)	76	—	
			24 (10)	24		
d	6 (1)	51	3.9 (8)	41	6.3 (5)	
	20 (3)	49	16 (2)	59		
e	3.9 (3)	58	3.3 (3)	65	6.0 (3)	82
	18 (2)	42	17 (2)	35	57 (10)	18
f	4.6 (3)	68	3.3 (3)	66	2.6 (3)	41
	24 (3)	32	17 (2)	34	12.4 (8)	59
g	4.0 (9)	65	1.4 (4)	31	8.7 (4)	
	17 (6)	35	13 (1)	69		
h	15 (2)		3 (1)	41	31 (3)	
			29 (7)	59		
i	6 (2)	20	10 (2)	52	37 (3)	
	39 (4)	80	60 (20)	48		
m	—		—		120 (10)	
n	—		—		11 (2)	53
					210 (70)	47
o	—		—		1.6 (3)	12
					22 (2)	47
					155 (15)	41

$T_{1\rho}$ values cannot give insight on molecular motion. Fortunately, in non-crystalline materials, like the elastomeric phases of the samples under study, the main contribution arises from spin-lattice relaxation and thus the ^{13}C $T_{1\rho}$ s are highly informative on mid-kHz motions²⁸; since these motions often correlate with the mechanical properties of polymers^{6,24}, these relaxation times are of great relevance in understanding the relationship between the macroscopic behaviour of these materials and their microscopic properties.

In the past, several authors^{11,29} have observed a non-exponential decay of the magnetization vs carbon spin-lock time curve: this was attributed to a distribution of relaxation times, ascribable to a distribution of correlation times and possibly to the presence of dynamic heterogeneity¹¹. In our systems most cases are well described by a two-exponential curve (see Table 6), as previously found, for instance, for the protonated carbons of some poly(ethylene terephthalate) yarns³⁰. A single decay constant was obtained for those peaks which show either a bad signal-to-noise ratio in the spectra or a relevant superposition by stronger peaks: the single relaxation time determined in these cases is probably an intermediate value between two relaxation times. For elastomeric phases, where the high mobility renders the presence of motional heterogeneities quite unlikely, the bi-exponential trend can be attributed to the presence of different mid-kHz motions with different correlation times.

The experimental data reported in Table 6 clearly indicate a noticeable difference between the elastomeric

and the crystalline phases. The trend

$$T_{1\rho} (\text{elastomeric phases}) < T_{1\rho} (\text{polypropylene}) \\ < T_{1\rho} (\text{polyethylene})$$

reflects the same trend observed for proton spin-lattice relaxation times in the rotating frame. Moreover, different $T_{1\rho}$ values for corresponding carbon nuclei in the elastomeric phases of the three samples are observed. For each carbon nucleus the following relationship holds:

$$T_{1\rho} (\text{EPR-Ti}) < T_{1\rho} (\text{EPDM}) < T_{1\rho} (\text{EPR-V}).$$

This indicates a different dynamical behaviour of the three samples in the kHz region, which differs from the MHz region (see ^{13}C T_1 data). This is in agreement with the ^1H $T_{1\rho}$ results obtained for EPR-V and EPDM (the values of the elastomeric phase in EPR-Ti were complicated by the presence of proton spin diffusion). Moreover, within each elastomeric phase, the different carbons, apart from the methyl ones, show similar $T_{1\rho}$ values. All this considered, the ^{13}C $T_{1\rho}$ values found in EPR-Ti for peak *e* are clearly different from those expected. The preliminary separation of the peaks, performed with the program 'SPORT-NMR', allows the exclusion of a contribution arising from the longer ^{13}C $T_{1\rho}$ s of peak *o*, which is partially superposed on peak *e*. Moreover, an analysis of the relative weights of the two relaxation times determined suggests that the shortest one (6 ms), which contributes 82% of the decay curve, arises from an average of the two relaxation times

normally found for the other peaks belonging to rubbery domains, whereas the longest one (57 ms) arises from a different phase, having reduced mobility in the mid-kHz region. Since the other peaks do not show relevant differences, this phase must be made of non-crystalline polyethylene and it seems logical to suppose that it is present either at the interface between the polyethylenic domains and the elastomeric matrix or between the crystalline lamellae. This hypothesis could explain the proton T_1 value obtained for peak *e*, which is slightly higher than those observed for the remaining peaks of the rubbery phase but noticeably smaller than the values found for the crystalline domains. In fact, the proton relaxation time of the rigid interfacial or inter-lamellar non-crystalline phase, which contributes to a small extent to the value observed for peak *e*, will be strongly influenced by spin diffusion from the crystalline neighbouring regions and is therefore expected to be larger than that of the rubbery phase.

Proton-carbon cross-polarization times. In order to gain further evidence of the presence of this interface, we measured the proton-carbon cross-polarization times for the different ^{13}C n.m.r. signals of EPR-Ti. In fact, since T_{CH} is sensitive to motions with long correlation times, it represents a useful tool for investigating the rigidity of a system³¹.

In the series of spectra obtained by varying the second contact pulse τ_2 in the IRCP sequence¹⁵ described in the Experimental section, the trend of the areas of the peaks ($M(\tau_2)$) vs the variable contact pulse, the expression for which can be obtained following Mehring³², was well fitted by a two-component curve for all the signals. The shortest component results in the range 200–400 μs for the rubber, contributing less than 8% of the signal, and approximately 20 μs for the crystalline phases, with a contribution of more than 60% of the signal. The longest component is of the order of some ms for the rubber and 300–400 μs for the crystalline phases. The values obtained for peak *e* are within the ranges found for the rubbery phase, the only difference being a higher contribution of the short component (approximately 15%); this is compatible with the presence of a rigid amorphous phase.

CONCLUSIONS

The structure, morphology and dynamics of an ethylene/propylene/ethylidene-norbornene terpolymer and two ethylene/propylene random copolymers obtained using different catalytic systems were characterized by carbon and proton solid-state n.m.r. measurements. The SPE-MAS spectra have yielded information on the primary structure of the random copolymers, indicating differences between the three samples investigated, and in particular as far as the regioregularity is concerned. Comparison between SPE-MAS and CP-MAS spectra, as well as static and selective experiments, have allowed us to single out and fully characterize the various phases of the different samples, supplying evidence that EPR-V and EPDM are monophasic rubbery systems whereas EPR-Ti is a heterophasic system consisting of polyethylene and polypropylene crystalline domains dispersed in a rubbery matrix. An estimate of a lower limit for the domain dimensions has been made on the basis of proton spin-lattice relaxation times. The

dynamics of the rubbery phases of the three samples has been examined by means of carbon relaxation times: small differences are observed in the motional behaviour in the MHz range, while stronger differences are found in the mid-kHz motions. Moreover, a thorough analysis of proton and carbon relaxation times and cross-polarization times has indicated the presence of a phase made of non-crystalline but quite rigid polyethylene at the interface between the polyethylenic domains and the elastomeric matrix, or between the crystalline lamellae.

ACKNOWLEDGEMENTS

M.G. thanks Montell for a PhD grant in Material Science. We also thank Dr P. Sgarzi (Centro Ricerche Montell 'G. Natta') for TEM analysis.

REFERENCES

1. Axelson, D. E., *J. Polym. Sci., Polym. Phys. Edn*, 1982, **20**, 1427.
2. Axelson, D. E., Mandelkern, L., Popli, R. and Mathieu, P., *J. Polym. Sci., Polym. Phys. Edn*, 1983, **21**, 2319.
3. McFaddin, D. C., Russel, K. E. and Kelusky, E. C., *Polym. Commun.*, 1986, **27**, 204.
4. Colquhoun, I. J. and Packer, K. J., *Br. Polym. J.*, 1987, **19**, 151.
5. Cudby, M. E. A., Harris, R. K., Metcalfe, K., Packer, K. J. and Smith, P. W. R., *Polymer*, 1985, **26**, 169.
6. Clayden, N. J., *Polymer*, 1992, **33**, 3145.
7. Clayden, N. J., *J. Polym. Sci., Polym. Phys. Edn*, 1994, **32**, 2321.
8. Carman, C. J., Harrington, R. A. and Wilkes, C. E. *Macromolecules*, 1977, **10**, 536.
9. Torchia, D. A., *J. Magn. Reson.*, 1978, **30**, 613.
10. Weiss, G. H., Gupta, R. K., Ferretti, J. A. and Becker, E. D., *J. Magn. Reson.*, 1980, **37**, 369.
11. Schaefer, J., Stejskal, E. O. and Buchdahl, R., *Macromolecules*, 1977, **10**, 384.
12. Kitamaru, R., Horii, F. and Murayama, K., *Macromolecules*, 1986, **19**, 636.
13. Stejskal, E. O., Schaefer, J., Sefcik, M. D. and McKay, R. A., *Macromolecules*, 1981, **14**, 275.
14. Tekely, P., Canet, D. and Delpuech, J. J., *Mol. Phys.*, 1989, **67**, 81.
15. Cory, D. G. and Ritchey, W. M., *Macromolecules*, 1989, **22**, 1611.
16. Geppi, M., Forte, C. and Ambrosetti, R., to be published.
17. Nielsen, N. C., Sangill, R., Bildsøe, H. and Jacobsen, H. J., *Macromolecules*, 1995, **28**, 2009.
18. Earl, W. L. and VanderHart, D. L., *Macromolecules*, 1979, **12**, 762.
19. Bunn, A., Cudby, M. E. A., Harris, R. K., Packer, K. J. and Say, B. J., *Polymer*, 1982, **23**, 694.
20. Havens, J. R. and VanderHart, D. L., *Macromolecules*, 1985, **18**, 1663.
21. Henrichs, P. M., Tribone, J., Massa, D. J. and Hewitt, J. M., *Macromolecules*, 1988, **21**, 1282.
22. Cheung, T. T. P., Gerstein, B. C., Ryan, L. M., Taylor, R. E. and Dybowski, C. R., *J. Chem. Phys.*, 1980, **73**, 6059. Cheung, T. T. P., *Phys. Rev. B*, 1981, **23**, 1404.
23. Cheung, T. T. P. and Gerstein, B. C., *J. Appl. Phys.*, 1981, **52**, 5517.
24. Voelkel, R., *Angew. Chem. Int. Ed. Engl.*, 1988, **27**, 1468.
25. Bovey, F. A. and Jelinski, L. W., *J. Phys. Chem.*, 1985, **89**, 571.
26. Gabrys, B., Horii, F. and Kitamaru, R., *Macromolecules*, 1987, **20**, 175.
27. Schröter, B. and Posern, A., *Makromol. Chem. Rapid Commun.*, 1982, **3**, 623.
28. Schaefer, J., Stejskal, E. O., Steger, T. R., Sefcik, M. D. and McKay, R. A., *Macromolecules*, 1980, **13**, 1121.

29. Le Menestrel, C., Kenwright, A. M., Sergot, P., Lauprêtre, F. and Monnerie, L., *Macromolecules*, 1992, **25**, 3020.
30. Gabriëse, W., Angad, Gaur, H., Feyen, F. C. and Veeman, W. S., *Macromolecules*, 1994, **27**, 5811.
31. Parker, A. A., Marcinko, J. J., Shieh, Y. T., Hedrick, D. P. and Ritchey, W. M., *J. Appl. Polym. Sci.*, 1990, **40**, 1717.
32. Mehring, M., *Principle of High Resolution NMR in Solids*. Springer-Verlag, Berlin, 1983.